$^{12,13}C(p,\pi^-)^{13,14}O_{g.s.}$ reactions in the Δ_{1232} resonance region

K. Hatanaka,[1,*] J. Kamiya,[1] D. Hirooka,[1] Y. Maeda,[1] Y. Maeda,[2] T. Noro,[1,†] E. Obayashi,[1] H. Okamura,[3] H. Sakai,[2] A. Tamii,[2] K. Tamura,[4] T. Wakasa,[1] K. Yako,[2] and H. P. Yoshida[1]
[1]*Research Center for Nuclear Physics, Osaka University, Ibaraki, Osaka 567-0047, Japan*
[2]*Department of Physics, University of Tokyo, Bunkyo, Tokyo 113-0033, Japan*
[3]*Department of Physics, Saitama University, Saitama 338-8570, Japan*
[4]*Department of Physics, Fukui Medical University, Fukui 910-1193, Japan*
(Received 10 January 2001; published 20 December 2001)

The role of the Δ resonance has been discussed for the $^{12,13,14}C(p,\pi^-)^{13,14,15}O_{g.s.}$ reactions both experimentally and theoretically. Recent calculations suggested resonance effects in the energy dependence of the differential cross section that seem to contradict existing data. Since the available data points are limited, it is important to measure the energy dependence of the differential cross sections and the analyzing powers in order to better understand the still unclear reaction mechanism of the ground state (p,π^-) reactions. In the present paper, angular distributions of the differential cross sections and the analyzing powers were measured for $^{12,13}C(p,\pi^\pm)$ reactions at incident energies of 250, 300, and 350 MeV. Experimental results for the $^{12}C(p,\pi^-)^{13}O_{g.s.}$ reaction are compared with full-range distorted-wave Born approximation calculations.

DOI: 10.1103/PhysRevC.65.014609 PACS number(s): 25.40.Qa, 27.20.+n, 24.10.Eq, 21.60.Cs

I. INTRODUCTION

Negative pion production in nuclei has been extensively studied over the past two decades. In particular, the role of the Δ_{1232} resonance has been discussed from both the experimental and theoretical point of view. Huber *et al.* [1] compared the energy dependence of the (p,π^-) and (p,π^+) reactions on ^{13}C leading to isobaric analog states of ^{14}O and ^{14}C at 250, 354, and 489 MeV. The differential cross sections of the (p,π^+) reactions are enhanced in the region of the resonance, similarly to those observed in the elementary $pp\rightarrow d\pi^+$ reaction. On the other hand, differential cross sections observed in the (p,π^-) reactions decrease with increasing energy. The (p,π^-) reaction is considered to be a two-nucleon process $(NN\rightarrow NN\pi^-)$, which means the incident proton interacts only with one of the neutrons in the target nucleus [2]. Huber *et al.* [1] discussed the lack of an enhancement at the invariant mass of the Δ_{1232} resonance as compared to what is expected on the basis of a phase shift analysis of differential cross sections for low-energy π^- absorption by a $^1S_0$, $T=1$ proton pair in ^3He [3]. These discrepancies suggest the need for the development of theoretical models and further experimental work in order to clear up questions about the sensitivity of the energy dependence of the (p,π^-) reaction to momentum transfer and to nuclear structure effects.

From a theoretical point of view, distorted-wave impulse approximation (DWBA) calculations within the two-nucleon model succeeded in explaining the overall features of the angular distributions of the differential cross sections and the analyzing powers for stretched state (p,π^-) transitions [4–6]. Within the same framework, Nose-Togawa *et al.* [7] investigated the energy dependence of the differential cross section for the $^{13}C(p,\pi^-)^{14}O_{g.s.}$ reaction and predicted a resonance structure around 300 MeV. The paucity of experimental data makes it difficult to clarify the discrepancies between existing data and theoretical predictions. Complete sets of angular distributions of the differential cross sections and the analyzing powers that are very important for the study of pion distortions have not been measured at 300 MeV. The work herein was motivated by theoretical attempts [7] to understand the underlying reaction mechanism, especially the role of the Δ resonance in (p,π^-) reactions. We measured a wide range of angular distributions of the differential cross sections and the analyzing powers for the (p,π^-) reactions on $^{12,13}C$ leading to oxygen ground states for bombarding energies of 250, 300, and 350 MeV. We also measured these distributions for (p,π^+) reactions to check the consistencies of the present measurements with existing data [1,8,9].

II. EXPERIMENT

The experiment was performed at the Research Center for Nuclear Physics (RCNP), Osaka University. Polarized protons from the atomic beam-type polarized ion source [10] were accelerated by the AVF and the ring cyclotrons. The beam intensity was 10–500 nA. The beam polarization was about 0.7, which was continuously monitored by an in-line polarimeter downstream of the ring cyclotron. The proton spin was flipped every second. Natural C and enriched ^{13}C (99%) targets were used. Target thicknesses were measured by weighing and were 87 and 136 mg/cm^2, respectively. The uncertainty in target thicknesses estimated to be $\pm 3.5\%$ was determined by comparing the measured differential cross sections for proton elastic scattering with existing data at 300 MeV [11]. Pions were momentum analyzed by the large acceptance spectrometer [12] (LAS) shown in Fig. 1. The horizontal and vertical acceptance was limited by slits to ± 50 and ± 60 mrad, respectively. The focal plane counter system consists of two vertical drift chambers (VDCs) for ray tracing and two ΔE trigger scintillators. Each VDC consists of pairs of x and u planes. Since the differential cross sections

*Electronic address: hatanaka@rcnp.osaka-u.ac.jp
†Present address: Department of Physics, Kyushu University, 6-10-1 Hakozaki, Higashi-ku, Fukuoka 812-8581, Japan.

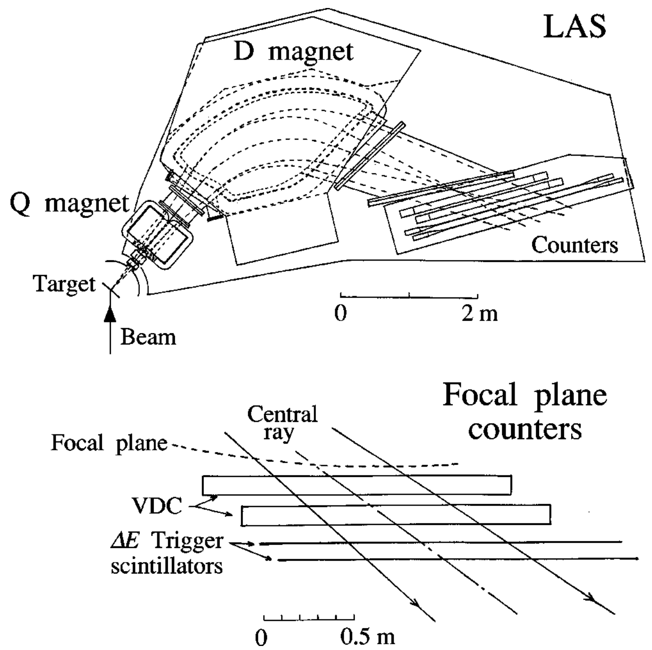

FIG. 1. Experimental setup of the LAS spectrometer and the focal plane counter system.

of (p,π) reactions are small, a second level trigger from the x plane of the first VDC in addition to the first level trigger derived from the coincidence of the two scintillators was employed to improve the signal-to-noise ratio. The resulting signal-to-noise ratio was improved typically by an order of magnitude from 2 to 20. The deadtime of the data acquisition system was typically 10%, and the data were correspondingly corrected in order to obtain the final yields. In the off-line analysis, the particle identification was performed by the two ΔE signals and the time of flight (TOF) through the spectrometer. Electrons and most of $\mu^{\pm}$ particles were rejected by the TOF gate. Events from these particles were uniformly distributed in the position spectrum at the focal plane and the resulting continuous background could be subtracted from the peaks. Particle trajectories were traced back from the focal plane to the entrance slit of LAS using transfer matrices, and a software cut was performed on the scattering angles in the horizontal plane. In the vertical plane, this procedure was not applied, since the vertical magnification is large and has insufficient angular resolution. Placement of this gate in the horizontal plane reduced the background, most of which were $\mu^{\pm}$ particles from decaying pions in flight, by about 20%. The combination of TOF and horizontal plane cuts produced typical peak to background ratios 50 and 25 for the (p,π^+) and (p,π^-) reactions, respectively. The efficiency of each plane of VDCs was estimated to be better than 90%, and the overall systematic uncertainties in the normalization were estimated to be less than 5%.

The energy resolution of the (p,π) reactions mainly due to the energy spread of the proton beam from the cyclotron was typically 400 keV full width at half maximum that was good enough to separate transitions to the ground state from excited state transitions.

TABLE I. Summary of measured differential cross sections of $^{12,13}C(p,\pi^+)$ reactions leading to ground states of $^{13,14}C$. All quantities shown are in the center-of-mass frame; angles are in degrees and $d\sigma/d\Omega$ are in nb/sr. The numbers in parentheses reflect statistical uncertainties only.

$^{12}C(p,\pi^+)$		$^{13}C(p,\pi^+)$	
$\theta_{c.m.}$	$^{13}C_{g.s.}$	$\theta_{c.m.}$	$^{14}C_{g.s.}$
	$T_p = 250$ MeV		
26.8[a]	632(56)	26.7[a]	247(31)
31[b]	331(36)	31[d]	127(14)
37.5[a]	273(34)	37.3[a]	105(13)
48.1[a]	140(18)	47.8[a]	37.1(4.8)
49.6[c]	96.4(16)	52[d]	27.6(3.3)
57.3[a]	60.7(5.5)	57.0[a]	16.9(2.3)
62[b]	29.1(4.1)		
63.7[c]	52.8(3.5)		
68.9[a]	27.3(3.6)		
	$T_p = 350$ MeV		
22[b]	157(14)	30[d]	57.9(6.4)
27.0[a]	106(15)	32.1[a]	39.6(9.3)
32[b]	106(11)	37[d]	42.3(5.1)
32.3[a]	100(19)	42.7[a]	14.3(3.5)

[a]Present work.
[b]Reference [9].
[c]Reference [8].
[d]Reference [1].

III. RESULTS AND DISCUSSION

Values of the differential cross sections for the (p,π^+) reactions at forward angles are compared with existing data in Table I. They are generally consistent with each other, taking into account the relatively large systematic uncertainties. The present results add considerably to the published data set that is quite sparse in places. The analyzing powers measured in the present work agree quite well with those for the $^{12}C(p,\pi^+)$ reaction at 250 MeV [8]. Angular distributions of the measured differential cross sections and the analyzing powers are shown in Fig. 2 for the $^{13}C(p,\pi^-)^{14}O_{g.s.}$ reactions. They are plotted as a function of the relativistically invariant Mandelstam variable t, which is defined as the square of the four-momentum transfer. The advantage of these t plots is that the nuclear structure effects are fixed in first order, and distributions reflect the reaction mechanism only. In the figure, it can be seen that the overall features for the (p,π^-) reactions do not change in the measured energy region.

In Fig. 3, angular distributions of the differential cross sections and the analyzing powers for the $^{12}C(p,\pi^-)^{13}O_{g.s.}$ reactions are compared with the DWBA calculations by Nose-Togawa [13]. The measured analyzing powers have positive values at all three energies and are quite different from those at 200 MeV [14]. From Figs. 2 and 3, one can see that the analyzing powers are clearly isotope dependent. The struck neutrons are in the $p_{3/2}$ and $p_{1/2}$ shells for ^{12}C and ^{13}C targets, respectively. In the calculations, distorted waves for incident protons were generated with optical potentials that

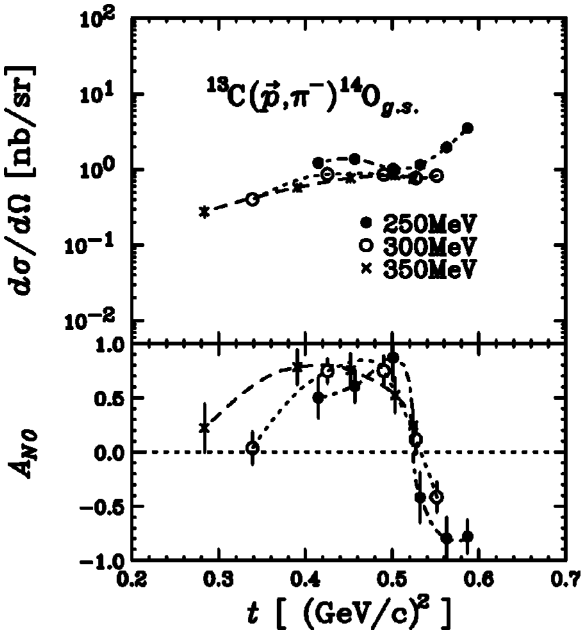

FIG. 2. t distributions of the differential cross sections and the analyzing powers for the ^{13}C$(p,\pi^-)^{14}$O$_{g.s.}$ reaction at 250, 300, and 350 MeV. Curves are to guide the eye.

describe the elastic scattering. The MSU optical potential was adopted for pions [15]. For the nuclear wave functions for ^{12}C and ^{13}O nuclei, $1p$-shell wave functions of Cohen-Kurath were employed [16]. Two-nucleon processes were taken into account as in the previous studies for stretched state transitions [4–6]. The s-wave rescattering process was neglected and only p-wave rescattering diagrams with π and ρ exchange were included in the calculations, since the present incident proton energies are well-above the threshold. The amplitude for the p-wave rescattering diagram is given by [7]

$$M_{ij}^{(p)}=\frac{f_\pi^*}{m_\pi}(\mathbf{S}_j\cdot\mathbf{k})(-)^\alpha T_j^{-\alpha}[V_\pi(q)+V_\rho(q)]D_\Delta, \quad (1)$$

where D_Δ is the Δ propagator, and V_π and V_ρ are given by

$$V_\pi(q)=\frac{f_\pi(q^2)f_\pi^*(q^2)}{m_\pi^2}(\sigma_i\cdot\mathbf{q})(\mathbf{S}_j^\dagger\cdot\mathbf{q}) \times(\tau_i\cdot\mathbf{T}_j^\dagger)\frac{-1}{(2\pi)^3(\mathbf{q}^2-q_0^2+m_\pi^2)}, \quad (2)$$

and

$$V_\rho(q)=\frac{f_\rho(q^2)f_\rho^*(q^2)}{m_\rho^2}(\sigma_i\times\mathbf{q})(\mathbf{S}_j^\dagger\times\mathbf{q}) \times(\tau_i\cdot\mathbf{T}_j^\dagger)\frac{-1}{(2\pi)^3(\mathbf{q}^2-q_0^2+m_\rho^2)}. \quad (3)$$

Here, the static form is used for the πNN vertex and the nucleon recoil terms were neglected. The transition spin and isospin operators are denoted by $\mathbf{S}$ and $\mathbf{T}$, respectively. Form factors are assumed as follows:

$$f_{\pi,\rho}(q^2)=f_{\pi,\rho}\frac{\Lambda_{\pi,\rho}^2-m_{\pi,\rho}^2}{\Lambda_{\pi,\rho}^2-q_0^2+\mathbf{q}^2},$$

$$f_{\pi,\rho}^*(q^2)=f_{\pi,\rho}^*\frac{\Lambda_{\pi,\rho}^{*2}-m_{\pi,\rho}^2}{\Lambda_{\pi,\rho}^{*2}-q_0^2+\mathbf{q}^2}. \quad (4)$$

Theoretical values overestimate the experimental cross sections at forward angles by about one or two orders of magnitude and calculated cross sections are renormalized to the data by factors indicated in Fig. 3. The present two-nucleon model reproduces the experimental flat angular distribution of the (p,π^-) differential cross section at 250 MeV. Normalized at forward angles, however, the DWBA results underestimate the data at backward angles and for higher energies. The measured analyzing powers show little energy dependence. On the other hand, the calculated values become positive and larger with increasing incident proton energies, which is consistent with previous results [7].

Figure 4 shows the energy dependence of the differential cross section at a constant value of $t=0.5\,(\mathrm{GeV}/c)^2$ plotted vs the center of mass energies ($\sqrt{s}$-$m_{12,13\mathrm{C}}$). Huber *et al.* [1] measured the cross section of the ^{13}C$(p,\pi^-)^{14}$O$_{g.s.}$ reaction at two angles for $T_p=250\,\mathrm{MeV}$ and at only one angle for 354 and 489 MeV. They applied the same relative normalization in exponential fits to the angular distributions at all three energies and at $t=0.5\,(\mathrm{GeV}/c)^2$ obtained cross sections of 1.6, 1.6, and 0.6 nb/sr for incident energies of 250, 354, and 489 MeV, respectively. The difference between the present data and these values stretches the systematic error bars to the limit. As can be seen in Fig. 4, the DWBA calculation predicts a large enhancement of the cross section near the invariant mass of the Δ_{1232} resonance, which is not seen in the present measurements. Calculated values are normalized by the factor of 0.057 and 0.045 for the reaction on ^{12}C and ^{13}C, respectively. Here, we assumed the overall normalization factors are independent of energy. For the positive pion production process $p+p\rightarrow p+n+\pi^+$, the dominant channel is $pp(^1D_2)\rightarrow N\Delta(^5\mathrm{S}_2)\rightarrow NN(^3\mathrm{S}_1)+\pi^+(p$ wave$)$, where the S wave intermediate $N\Delta$ and the final NN states are involved. For the negative pion production, the short-range nature of the (p,π^-) process also favors a relative S state for the final two protons ($^1\mathrm{S}_0$). If we assume the dominant final $pp(^1\mathrm{S}_0)$ channel and also a pion orbital angular momentum of 0 or 1, only the $N\Delta(^3\mathrm{P}_0)$ intermediate state is allowed. The phase shift analysis of the $\pi^-pp(^1\mathrm{S}_0)\rightarrow pn$ angular distribution extracted from the ^{3}He$(\pi^-,pn)n$ data suggests that the reaction proceeds via $\pi^-pp(^1\mathrm{S}_0)\rightarrow pn$ ($^3\mathrm{S}_1$ and $^3\mathrm{D}_1$, $T=0$) where the intermediate $N\Delta$ state is forbidden [17]. Similar results were reported from the partial wave amplitude analysis of the analyzing powers for the $\vec{p}n\rightarrow pp(^1\mathrm{S}_0)\pi^-$ reaction [18]. In the present measurements the energy dependence of the differential cross sections for the (p,π^+) reactions is consistent with previously reported Δ resonance effects [1,9]. On the other hand, it is confirmed that nonresonant processes dominate the ^{12,13}C(p,π^-) reactions leading to their respective ground states. Theoretical studies are expected to clarify the role of the s-wave rescattering process even at energies well-above the threshold. The

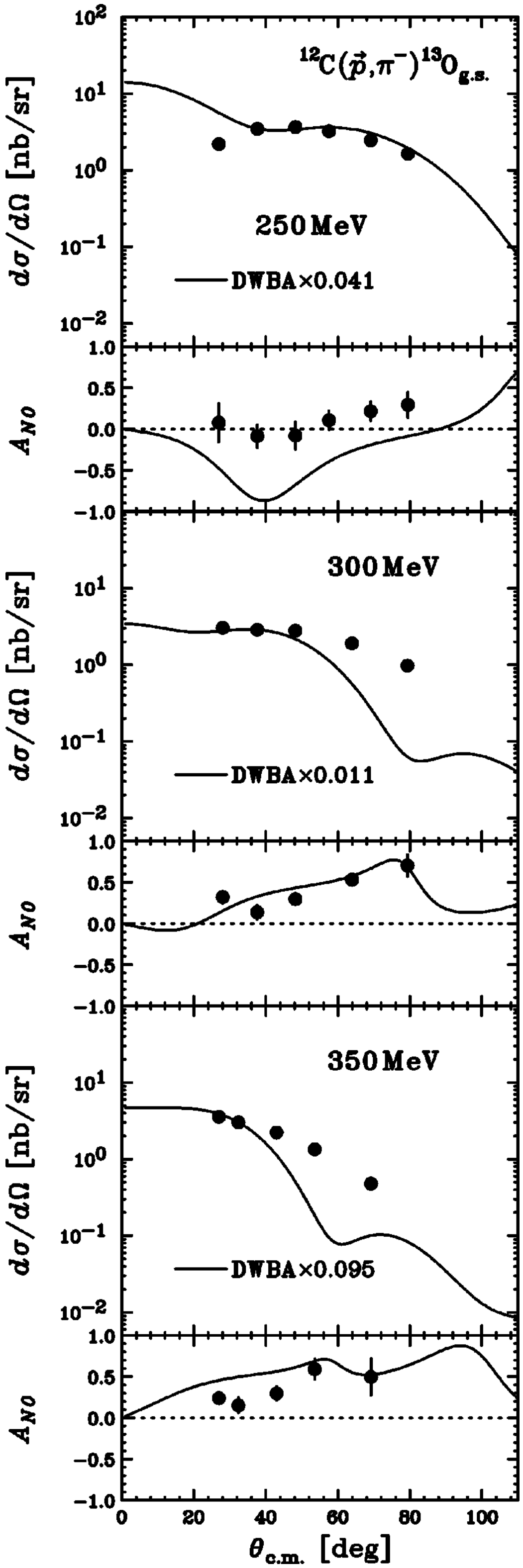

FIG. 3. Angular distributions of the differential cross sections and the analyzing powers for $^{12}C(p,\pi^-)^{13}O_{g.s.}$ reactions at 250, 300, and 350 MeV. Solid curves are the DWBA results described in the text. For cross sections, calculated values are multiplied by the factors in the figure.

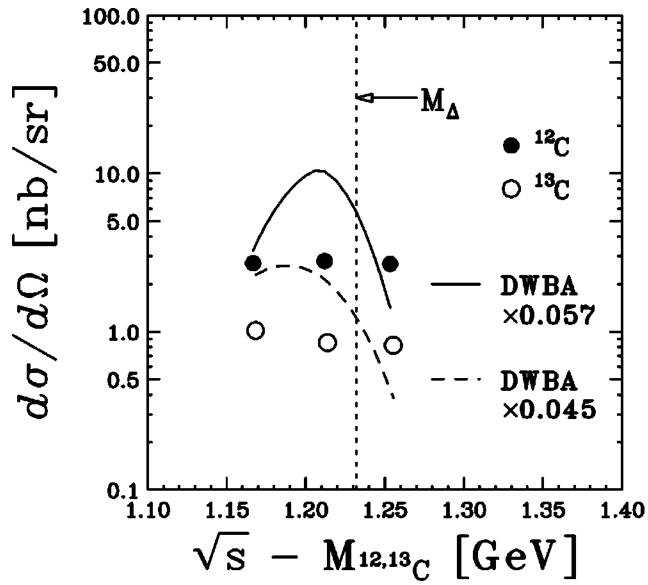

FIG. 4. The energy dependence of the differential cross sections at a constant value of $t=0.5$ $(\mathrm{GeV}/c)^2$ plotted vs the center-of-mass energies ($\sqrt{s}-m_{12,13_C}$). Filled and open circles are results for ^{12}C and ^{13}C, respectively. The solid curve shows calculations for the $^{12}C(p,\pi^-)$ reaction that is multiplied by 0.057. The dashed curve shows calculations for the $^{13}C(p,\pi^-)$ reaction that is multiplied by 0.045.

present analyzing power data are useful in ascertaining pion distortion effects.

IV. SUMMARY

We have measured angular distributions of the differential cross sections and the analyzing powers for $^{12,13}C(p,\pi^{\pm})$ reactions leading to ground states of the residual nuclei at incident energies of 250, 300, and 350 MeV. This is the first measurement covering a wide angular range in the Δ_{1232} resonance region. Experimental results for the $^{12}C(p,\pi^-)^{13}O_{g.s.}$ reaction were compared with full-range DWBA calculations based on the two-nucleon model that explained the overall features of the angular distributions of the differential cross sections and the analyzing powers for stretched state transitions near threshold energies. The DWBA calculations failed to reproduce the ground state transitions. The measured energy dependence of the differential cross sections confirmed that the nonresonant processes dominate the $^{12,13}C(p,\pi^-)^{13,14}O_{g.s.}$, transitions at the Δ_{1232} resonance region.

ACKNOWLEDGMENTS

We thank the RCNP staff for their continuous support during the experiment. We also wish to thank Professor H. Toki and Professor K. Kume for helpful discussions and Dr. N. Nose-Togawa for the results of her calculations that she made available to us along with her very useful comments. We are grateful to Dr. G. P. A. Berg and Dr. M. B. Greenfield for their critical reading of the manuscript. This experiment was performed under Program No. E125 at RCNP.

[1] G. M. Huber, G. J. Lolos, R. D. Bent, K. H. Hicks, P. L. Walden, S. Yen, X. Aslanoglou, E. G. Auld, and W. R. Falk, Phys. Rev. C **37**, 1161 (1988).
[2] S. E. Vigdor, T. G. Throwe, M. C. Green, W. W. Jacobs, R. D. Bent, J. J. Kehayias, W. K. Pitts, and T. E. Ward, Nucl. Phys. **A396**, 61c (1983).
[3] E. Piasetzky, D. Ashery, M. A. Moinester, G. A. Miller, and A. Gal, Phys. Rev. Lett. **57**, 2135 (1986).
[4] K. Kume, Nucl. Phys. **A504**, 712 (1989).
[5] K. Kume, Nucl. Phys. **A511**, 701 (1990).
[6] N. Nose, K. Kume, and H. Toki, Phys. Rev. C **53**, 2324 (1996).
[7] N. Nose-Togawa, K. Kume, and H. Toki, Phys. Rev. C **57**, 2502 (1998).
[8] G. J. Lolos, E. G. Auld, W. R. Falk, G. L. Giles, G. Jones, B. J. McParland, R. B. Taylor, W. Ziegler, and P. L. Walden, Phys. Rev. C **30**, 574 (1984).
[9] G. M. Huber, G. J. Lolos, E. L. Mathie, Z. Papandreou, K. H. Hicks, P. L. Walden, S. Yen, X. Aslanoglou, E. G. Auld, and W. R. Falk, Phys. Rev. C **36**, 1058 (1987).
[10] K. Hatanaka, K. Takahisa, H. Tamura, M. Sato, and I. Miura, Nucl. Instrum. Methods Phys. Res. A **384**, 575 (1997).
[11] H. Sakaguchi *et al.*, RCNP report, 1993.
[12] N. Matsuoka, T. Noro, K. Sagara, S. Morinobu, A. Okihana, and K. Hatanaka, RCNP report, 1992.
[13] N. Nose-Togawa (private communication).
[14] W. W. Jacobs, T. G. Throwe, S. E. Vigdor, M. C. Green, J. R. Hall, H. O. Meyer, W. K. Pitts, and M. Dillig, Phys. Rev. Lett. **49**, 855 (1982).
[15] M. Gmitro, S. S. Kamalov, and R. Mach, Phys. Rev. C **36**, 1105 (1987).
[16] S. Cohen and D. Kurath, Nucl. Phys. **73**, 1 (1965).
[17] H. Hahn, A. Altman, D. Ashery, G. Gefen, D. R. Gill, R. R. Johnson, R. Levy-Nathansohn, M. A. Moinester, M. Sevior, and R. P. Trelle, Phys. Rev. C **53**, 1074 (1996).
[18] H. Hahn *et al.*, Phys. Rev. Lett. **82**, 2258 (1999).